◆ Human Brain Mapping 37:4640–4653 (2016) ◆

Impairment in Subcortical Suppression in Schizophrenia: Evidence from the fBIRN Oddball Task

Katie M. Lavigne,[1,2] Mahesh Menon,[1] and Todd S. Woodward[1,2]*

[1]*Department of Psychiatry, University of British Columbia, Vancouver, British Colombia, Canada*
[2]*BC Mental Health and Addictions Research Institute, Provincial Health Services Authority, Vancouver, British Colombia, Canada*

Abstract: Schizophrenia patients show widespread impairments in brain activity during oddball tasks, which involve responding to infrequent target stimuli while refraining from responding during continuous non-target stimuli. In a network-based investigation comparing schizophrenia or schizoaffective patients to healthy controls, we sought to clarify which networks were specifically associated with target detection using a multivariate analysis technique that identifies task-specific functional brain networks. We acquired data from the publicly available function biomedical informatics research network collaboration, including 58 patients and 50 controls. Two task-based functional brain networks were identified: (1) a response modulation network including bilateral temporal pole, supramarginal gyrus, striatum, and thalamus, on which patients showed decreased activity relative to controls; and (2) an auditory–motor response activation network, on which patients showed a slower return to baseline than controls, but no difference in peak activation. For both groups, baseline to peak activation of the response modulation network correlated negatively with peak to baseline activity in the response activation network, suggesting a role in suppressing the motor response following targets. Patients' impaired activity in the response modulation network, and subsequent longer return to baseline in the response activation network, correspond with their later and less accurate behavioral performance, suggesting that impairment in suppression of the auditory–motor response activation network could underlie oddball task deficits in schizophrenia. In addition, the magnitude of the activity in the response modulation network was correlated with intensity of delusions of reference, supporting the notion that increased referential ideation is associated with hyperactivity within the subcortical striatal–limbic network. *Hum Brain Mapp 37:4640–4653, 2016.* © 2016 Wiley Periodicals, Inc.

Key words: schizophrenia; target detection; functional magnetic resonance imaging; functional connectivity

The authors report no potential conflicts of interest.
*Correspondence to: Todd S. Woodward, Ph. D.; Room A3-A117, BC Mental Health & Addictions Research Institute – Translational Research Building, 3rd Floor, 938 W. 28th Avenue, Vancouver, British Columbia, Canada, V5Z 4H4. E-mail: todd.s.woodward@gmail.com

Received for publication 18 November 2015; Revised 20 July 2016; Accepted 22 July 2016.
DOI: 10.1002/hbm.23334
Published online 1 August 2016 in Wiley Online Library (wileyonlinelibrary.com).

© 2016 Wiley Periodicals, Inc.

INTRODUCTION

Schizophrenia patients show widespread impairments in functional brain activity during oddball tasks, which index the ability to detect and orient toward salient environmental stimuli [Kiehl et al., 2005a]. Oddball tasks generally involve responding to infrequent deviant (target) stimuli interspersed among continuous standard (non-target) stimuli, to which no response should be made. These stimuli may be in different modalities (e.g., auditory, visual, tactile), but auditory stimuli usually consisting of tones of varying pitch are most common, especially in research involving schizophrenia patients. The most robust finding on oddball tasks and schizophrenia stems from the event-related potential (ERP) literature, with schizophrenia patients demonstrating a reliable and strong reduction in P300 relative to controls during target detection [Jeon and Polich, 2003]. The P300 ERP is a positive deflection elicited by novel salient stimuli, occurs approximately 300–600 ms poststimulus, and is thought to reflect context processing, salience detection, and working memory.

Source localization studies of P300 during oddball tasks have implicated widespread brain regions, including bilateral temporal cortex (for auditory stimuli), supplementary motor area/anterior cingulate cortex (SMA/ACC), supramarginal gyrus, and insula [Mangalathu-Arumana et al., 2012; Mulert et al., 2004; Soltani and Knight, 2000]. These source localization findings are in line with functional magnetic resonance imaging (fMRI) research; one study identified over 30 brain regions showing increased activity during target detection [Kiehl et al., 2005b]. Many of these regions overlap with those thought to underlie the P300 response; however, fMRI studies have also reported increased activity in subcortical regions [Cacciaglia et al., 2015; Kiehl et al., 2005b], including thalamus, putamen, amygdala, and brainstem, which are difficult to detect using scalp-based electrophysiological procedures. fMRI research on oddball tasks in schizophrenia has revealed that patients show reduced activity during target detection in many of these regions, including bilateral superior temporal gyrus, inferior parietal lobule, anterior/posterior cingulate cortex, insula, thalamus, and cerebellum [Gur et al., 2007; Kiehl and Liddle, 2001; Kiehl et al., 2005a].

Recently, the focus of neuroimaging research has shifted from examination of discrete brain regions to a more comprehensive network-based approach to understanding functional brain activity. To that end, researchers have identified several, sometimes distant, clusters of brain regions that function together as networks [Buckner et al., 2008; Fox et al., 2005; Raichle and MacLeod, 2001; Yeo et al., 2011]. Two networks of particular relevance to the oddball task are the dorsal and ventral attention networks [Corbetta and Shulman, 2002; Yeo et al., 2011]. The dorsal attention network includes the intraparietal sulci and frontal eye fields, and is involved in top-down orienting of attention. The ventral attention network, which includes the ACC, insula, and temporoparietal junction, is recruited when detecting salient environmental stimuli, and is involved in bottom-up attentional mechanisms. A recent meta-analysis [Kim, 2014] showed that regions of the ventral attention network were associated with target detection, whereas regions of the dorsal attention network were associated with both target and non-target trials, suggesting a more general involvement in sustained attention during performance of the task.

Network-based studies of oddball tasks in schizophrenia [Calhoun et al., 2006; Kim et al., 2009; Sakoglu et al., 2010] have identified several networks on which patients show hypoactivity relative to controls during target detection. In some cases, these networks overlap with the ventral attention network; however, other networks have also been implicated, such as the default-mode network, which is known to be affected in schizophrenia [Garrity et al., 2007; Lavigne et al., 2015b; Metzak et al., 2012; Woodward et al., 2016], as well as sensory-specific networks, such as auditory networks during auditory oddball tasks. Kim et al. [2009] suggested that hypoactivity in non-primary auditory cortex with relatively intact activation in primary auditory areas during oddball tasks reflects deficits in transitioning from primary to higher-order sensory processing in schizophrenia. Interestingly, Wynn et al. [2015] combined fMRI and EEG during visual oddball in schizophrenia, finding that P300 corresponded to activation in the ventral attention network during the task, and activity in both modalities was reduced in schizophrenia patients, suggesting that the ventral attention network underlies the P300 response, and particularly, the robust finding of reduced P300 in schizophrenia.

Most network-based fMRI studies on auditory oddball in schizophrenia have employed independent component analysis (ICA). ICA is a blind source separation technique that derives functional brain networks from variance reflecting overall brain activity, including activity that is unrelated to the task. Therefore, some of the functional brain networks observed, even when correlated with task timing post hoc, are not optimized to explain task-related activity. Constrained principal component analysis for fMRI [fMRI-CPCA; Lavigne et al., 2015a; Metzak et al., 2011; Woodward et al., 2013] addresses this limitation by deriving networks from task specific activations through the use of multivariate multiple regression followed by principal component analysis. This results in functional brain networks that are dependent on task timing and, therefore, task specific. In the current study, we acquired publicly available functional magnetic resonance imaging (fMRI) data from the function biomedical informatics research network (fBIRN) multisite collaboration [Friedman et al., 2008; Keator et al., 2008] to examine differences in task specific functional brain network activity between schizophrenia patients and healthy controls on an auditory oddball task. fMRI-CPCA was employed to identify task-related functional brain networks, and the estimated hemodynamic response within each network was compared across groups and testing sites.

TABLE I. Demographic information, symptoms, and performance on the auditory oddball task

Variable	Healthy controls	Schizophrenia patients
Demographics		
N	50	58
Gender (# male)	34	45
Handedness (# right)	48	53
Age (mean; SD)	34.88 (12.82)	37.57 (12.68)
Auditory oddball performance	**Mean (SD)**	**Mean (SD)**
Trials	29.00 (0.08)	28.99 (0.12)
Hits*	24.80 (4.76)	22.73 (5.40)
Errors	1.56 (2.81)	2.38 (3.60)
Late*	0.31 (0.56)	0.61 (0.89)
Missed	2.63 (3.33)	3.88 (4.11)
False Positives	1.26 (1.82)	1.72 (2.01)
Accuracy*	85.5%	78.54%
RT – Hits**	396.10 (62.59)	444.98 (84.48)
RT – Errors	450.53 (109.81)	494.54 (117.67)
RT – Late	1,181.17 (108.26)	1,170.93 (91.56)
Symptom ratings (patients only)	**Mean (SD)**	**Range**
Affective flattening	1.60 (1.75)	0–5
Alogia	0.97 (1.31)	0–4
Avolition-apathy	2.55 (1.34)	0–5
Anhedonia-asociality	2.60 (1.41)	0–5
Attention	0.86 (1.24)	0–5
Severity of hallucinations	2.16 (1.85)	0–5
Severity of delusions	2.38 (1.60)	0–5
Severity of bizarre behavior	0.83 (1.26)	0–4
Positive formal thought disorder	0.95 (1.38)	0–5

Note. RT, reaction time; SD, standard deviation; * = $P < 0.05$; ** = $P < 0.001$.

METHODS

Participants

The publicly available fBIRN phase II multi-site study consists of fMRI data collected at six different sites across the United States of America: Duke/UNC, Brigham and Women's Hospital (BWH), Massachusetts General Hospital (MGH), University of California—Irvine (UCI), University of New Mexico (UNM), and Yale. All sites received local Institutional Review Board approval. Data were downloaded from the Function BIRN Data Repository (http://fbirnbdr.birncommunity.org:8080/BDR/), Project Accession Number 2007-BDR-6UHZ1. Eighty-three patients (56 male; 74 right handed) diagnosed with schizophrenia or schizoaffective disorder and eighty healthy controls (66 male; 74 right handed) completed an auditory oddball task as part of a larger battery while undergoing fMRI. Both patients and controls were excluded if they had a history of major neurological or medical illness, head injury, substance or alcohol dependence, an IQ less than 75 as measured by the North American Adult Reading Test [NAART; Blair and Spreen, 1989], or were currently taking medications to treat migraines. Patients were interviewed by experienced raters using the Structured Clinical Interview for Diagnostic and Statistical Manual of Mental Disorders, Fourth Edition, Text Revision [DSM-IV-TR; First et al., 2002b] Axis I Disorders, Patient Edition, and those meeting criteria for either schizophrenia or schizoaffective disorder were included in the study. Patients with severe extrapyramidal symptoms or tardive dyskinesia were excluded. Healthy controls were interviewed using the Structured Clinical Interview for DSM-IV-TR Axis I Disorders, Non-patient Edition [First et al., 2002a], and were excluded if they had a current or past history of psychiatric illness, or if a first degree family member had a diagnosis of a psychotic illness. Patients' symptoms were measured with the Scales for the Assessment of Positive/Negative Symptoms [SAPS/SANS; Andreasen, 1984a,b]. Patients were clinically stable and had no changes in their medication use in the previous two months; however, more detailed information on medication history and dosage was not available.

Protocol Standardization and Quality Control

Although multisite studies provide many advantages, such as increased statistical power due to large sample sizes, differences in the scanning and assessment protocols used at each site can introduce unwanted variability into the data. It is, therefore, important to ensure experimental procedures are optimized and standardized across sites, and monitored throughout data collection. Prior to collection of the fBIRN Phase II data used in the current study, the fBIRN group conducted a preliminary traveling subjects study, in which subjects were scanned twice on consecutive days at each site, with the goal of assessing both test-retest and between-site reliability. This led to several recommendations for increasing reliability, including controlling for differences in field strength and scanning parameters across scanners [Friedman et al., 2006a,b, 2008], which were incorporated into Phase II data collection. Working groups were formed to (1) standardize fMRI calibration by identifying scanner differences and controlling for these at data acquisition through the use of a standardized protocol (see *Image Acquisition*), (2) create standard protocols and rater training for clinical assessments, and to (3) optimize procedures for the cognitive tasks used during data collection [Glover et al., 2012].

We implemented additional quality control procedures by assessing the images after each preprocessing step, excluding data on a run-by-run basis to retain the maximum possible data while still ensuring quality. However, we decided to exclude one site (UCI), which consisted of 42 participants (20 controls, 22 patients), due to errors during normalization to the EPI template provided by SPM in the majority of subjects/runs, which led to the exclusion of large portions of the brain from the overall mask during analysis. Excluding an entire site is not ideal, but is recommended if it leads to improvements in data quality

[Friedman et al., 2008]. About 170 additional runs were discarded due to: (1) images showing artifacts and/or leading to errors during preprocessing (99 runs; 11.4% of all runs); (2) responses made on less than 20% of trials (27 runs; 3.1%); (3) the number of false positives (responses made outside the response window) exceeding the number of responses within the response window (15 runs; 1.7%); and (4) head movement exceeding 3 mm or 3 degrees (29 runs; 3.3%). This led to the exclusion of 13 additional participants (10 controls, 3 patients) across all sites, leading to a final sample of 58 patients (47 schizophrenia, 6 schizoaffective, 5 missing SCID data) and 50 healthy controls. There were no significant group differences on age ($P > 0.27$) or gender ($P > 0.26$) in the final sample (see Table I).

Experimental Design

The auditory oddball paradigm (Fig. 1) consisted of a two-tone oddball task, in which participants were presented with a series of standard (1,000 Hz; 95% occurrence) and target (1,200 Hz; 5% occurrence) tones (tone duration = 100 ms, ISI = 500 ms), and were instructed to press a button with the index finger of their right hand in response to target tones. The time between two target tones (i.e., inter-trial interval) varied randomly between 6 and 15 s, allowing for deconvolution of the BOLD signal [Serences, 2004], and leading to approximately 30 trials per run. The start and end of each run was signaled by a 15 s silent fixation period, leading to a total run duration of 280 s. Participants completed up to 8 runs over two identical sessions with an interval of at least 24 hours and no more than 3 weeks between them. One control participant completed 12 runs over 3 sessions. Stimuli were presented using E-prime software (http://www.pstnet.com/products/e-prime/), and were delivered through headphones during the experimental sessions. The volume for right and left headphones was adjusted by the participant during a calibration scan such that tones could be heard comfortably over the scanner noise. Participants performed two practice runs in front of a computer monitor prior to the experimental sessions.

Image Acquisition

Imaging data was included from five sites: Duke/UNC (4T GE Lx); BWH (GE Signa 3T); MGH (Siemens 3T Trio); UNM (Siemens 1.5T Trio); and Yale (Siemens 3T Trio). Imaging parameters were matched as closely as possible between sites based on preliminary studies collected as part of the fBIRN multisite study [Friedman et al., 2008; Keator et al., 2008; Magnotta and Friedman, 2006; also see above): 27 slices when possible; thickness/gap = 4 mm/1 mm; matrix = 64 × 64; repetition time (TR) = 2,000 ms; echo time (TE) = 30 ms (3 T)/40 ms (1.5 T); flip angle (FA) = 90°; field of view (FOV) = 22 cm; voxel dimensions = 3.4375 × 3.4375 × 4 mm). One site (Duke/UNC) employed a spiral echo sequence, while all other sites used a single-shot EPI sequence. 140 volumes were collected in each run.

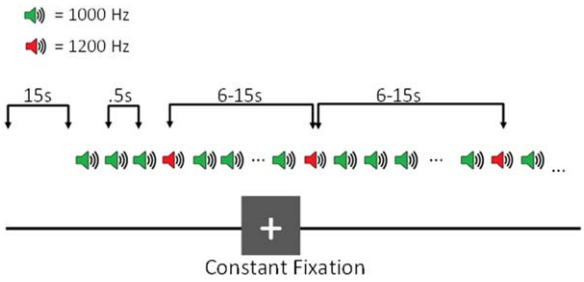

Figure 1.
Auditory Oddball Task: Experimental Design. Participants were presented with a series of standard (1,000 Hz) and deviant (1,200 Hz) tones, and were instructed to press a button in response to deviant tones. About 5% of the tones presented were deviant tones, and the time between two deviant tones ranged from 6 to 15 s. [Color figure can be viewed at wileyonlinelibrary.com]

Image Preprocessing

All functional images were preprocessed using Statistical Parametric Mapping 8 (SPM 8; Wellcome Trust Centre for Neuroimaging, United Kingdom). For each participant, each functional run was realigned, normalized to Montreal Neurological Institute (MNI) standard space using the EPI template provided by SPM, and subsampled to 2 mm^3. Data were spatially smoothed with an 8 mm full width at half maximum Gaussian filter.

Data Analysis

fMRI-CPCA

The following is a brief overview of the fMRI-CPCA methodology. For theory and proofs behind CPCA, see Hunter and Takane [2002] and Takane and Shibayama [1991]. More in-depth descriptions of CPCA as applied to fMRI data can be found in previously published work [Lavigne et al., 2015a; Metzak et al., 2011, 2012; Woodward et al., 2013]. The fMRI-CPCA application is available online, free of charge (www.nitrc.org/projects/fmricpca). fMRI-CPCA combines multivariate multiple regression and principal component analysis (PCA) to reveal multiple independent sources of poststimulus fluctuations in brain activity. The first step of fMRI-CPCA consists of a multivariate multiple regression, in which whole brain blood-oxygen-level dependent (BOLD) signal is regressed onto a matrix modeling stimulus timing, which serves to partition the overall variance into task-related (predictable) and task-unrelated (residual) fluctuations. This is achieved by

concatenating the preprocessed data into a single matrix, with one row for each subject- and run-specific whole brain scan, and one column for each voxel. This resulted in a matrix of 97,440 rows (108 subjects × up to 11 runs per subject × 140 scans per subject) by 585,390 columns (585,390 voxels in $2mm^3$ resolution) for the current study. The data matrix included both groups to allow for identification of networks potentially common to all subjects, and subsequent comparison of activity between groups. Non-brain areas were then masked out and the resulting data matrix underwent several transformations to improve quality; specifically, linear and quadratic effects as well as head motion parameters were regressed out, and the data were mean-centered and standardized. The data matrix was regressed onto a finite impulse response (FIR)-based design matrix detailing stimulus timing information. Like the data matrix, the design matrix consists of a single row for each subject- and run-specific whole brain scan; however, the columns code subject, condition, and post-stimulus timing information. Specifically, a value of 1 is placed in cells where hemodynamic response is to be estimated, and a value of 0 is placed everywhere else, creating mini-boxcar functions. For the current analysis, we modeled 7 poststimulus time points, or 14 s after the onset of the target stimulus (TR = 2). With 108 subjects and a single condition, this led to a design matrix of 974,40 rows and 756 columns (7 * 108 = 756). This first step results in a matrix of predicted scores, that is, the variance in the data matrix which is predictable from stimulus timing information. The second step involves submitting these predicted scores to a PCA, which results in orthogonal components reflecting functional brain networks that fluctuate as a function of stimulus timing.

Functional brain networks associated with each orthogonal source are spatially interpreted by examining the voxels whose activity dominated each component, and temporally interpreted by statistically assessing the hemodynamic response (HDR) shape associated with each component. In the current study, the PCA solution was submitted to an orthogonal rotation [Metzak et al., 2011] to enhance interpretability. fMRI-CPCA is able to (1) identify multiple functional brain networks simultaneously involved in executing a cognitive task, (2) estimate the poststimulus time course of coordinated BOLD activity fluctuations associated with each functional network for each subject, and (3) statistically test the effect of experimental manipulations and group differences on BOLD activity in each functional brain network.

Relation to Experimental Conditions

fMRI-CPCA produces predictor weights for each network and each combination of subject, condition, and poststimulus time. These predictor weights, which are the weights that would be applied to the FIR-based design matrix to compute the component scores, provide estimates of the engagement of functional networks over time for all subjects for each condition, and can be analyzed statistically to determine whether or not these values reflect a reliable HDR shape, and whether differences between groups and/or conditions exist within each network. This was achieved by submitting the predictor weights to a 7 × 2 × 2 mixed-model ANOVA, with the within-subjects factor of Poststimulus Time (7 time points were modeled after stimulus onset), and the between-subjects factors of Component (2 components were extracted) and Group (schizophrenia patients and healthy controls). Tests of sphericity were carried out, and corrections for violations of sphericity did not affect interpretation of the results; therefore, the original degrees of freedom are reported below.

Interrelationship between Brain Networks

Predictor weights also allow computation of relationships between functional brain networks. Different cognitive processes can underlie the magnitude of the baseline-to-peak versus post-peak-to-baseline trajectories of the task related HDR shape reflected by the predictor weights [Woodward et al., 2016]. Therefore, for each component, using the peak averaged over all subjects as a reference point, we computed two measures for each functional brain network: one baseline-to-peak (including the peak but not the starting scans) and a second post-peak back to baseline. These computed scores could then be intercorrelated to study positive and negative interactions between functional brain networks.

RESULTS

Behavioral

Table I displays means for accuracy and reaction times (RTs) for each group, as well as basic demographic and symptom information. Hits were correct responses made within 1 s of the target onset and errors were incorrect responses (either wrong response button used or multiple responses) made within the same time period. This 1s time window was defined by the fBIRN group and includes the first standard tone following a target; however, as can be seen in Table I, the average RT was within the 0.5 s following the target tone. Late responses were responses made between 1 and 1.5 s of the target onset (extended to the second standard tone following the target), and misses included target trials in which no response was made. Finally, false positives were responses made to standard tones.

Independent samples *t*-tests revealed that schizophrenia patients had significantly fewer hits, $t(106) = 2.10$, $P < 0.05$, and reduced accuracy, $t(106) = 2.06$, $P < 0.05$, relative to healthy controls. Patients also showed a significantly greater number of late responses, $t(97.58) = -2.11$, $P < 0.05$, and

slower hit RTs, $t(103.76) = -3.44$, $P < 0.001$, relative to healthy controls. There were no significant differences between groups on the number of trials, errors, misses, or false positives. There were also no significant group differences on RTs for errors or late responses.

Since patients showed fewer hits and more late responses than controls, and had slower hit RTs, we examined whether late responses could account for the significantly poorer accuracy in patients, by combining the number of hits and number of late responses into a composite variable. The difference between patients and controls was no longer significant with this new measure, and the modified accuracy score using this measure (i.e., [number of hits + number of late responses]/number of trials) also failed to reach significance. These results suggest that, compared with healthy controls, schizophrenia patients responded more slowly to target stimuli, which resulted in significantly poorer accuracy on the task.

fMRI-CPCA

Inspection of the scree plot of singular values [Cattell, 1966; Cattell and Vogelmann, 1977] suggested that two components should be extracted. Components 1 and 2 accounted for 26.23% and 12.21% of the variance that could be predicted from stimulus timing, respectively. Visual inspection of the predictor weights confirmed a hemodynamic response shape for both networks (Figs. 2B and 3B), and each showed a significant effect of Poststimulus Time, $F(6, 636) = 39.92$, $P < 0.001$, $F(6, 636) = 156.32$, $P < 0.001$, for Components 1 and 2, respectively, demonstrating a plausible and reliable HDR signal for each functional brain network [Metzak et al., 2011, 2012; Woodward et al., 2013]. Analysis of the HDR shapes with a 7 (Poststimulus time) × 2 (Component) × 2 (Group) mixed model ANOVA revealed a significant Component × Poststimulus Time × Group interaction, $F(6,636) = 7.50$, $P < 0.001$, suggesting that group differences depended on both Component and Poststimulus Time. This interaction was interpreted using two 7 (Poststimulus Time) × 2 (Group) mixed-model ANOVAs, one for each component.

Component 1

The brain regions associated with Component 1 are displayed in Figure 2A, with anatomical descriptions in Table II. This network included activations in bilateral temporal pole/anterior superior temporal gyrus (STG; BA 38), posterior middle temporal gyrus (MTG; BAs 20, 21, 37), anterior/posterior cingulate cortex (ACC/PCC; BAs 24, 23), occipital cortex (BAs 17, 18), supramarginal gyrus (BA 40), and several subcortical regions, including bilateral thalamus, striatum, hippocampus, amygdala, and cerebellum. There was a significant Poststimulus Time × Group interaction, $F(6, 636) = 7.03$, $P < 0.001$, and a significant main effect of Group, $F(1, 106) = 7.05$, $P < 0.01$. Follow up simple

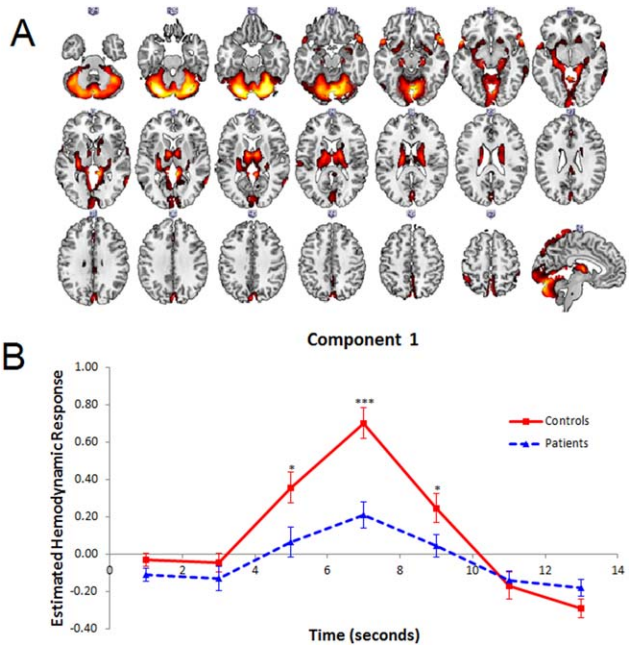

Figure 2.

(**A–C**) (A) Dominant 10% of component loadings for Component 1 Response Modulation (red/yellow = positive loadings, threshold = 0.07, max = 0.11; no negative loadings passed threshold). Overlapping regions are displayed in pink/white. Montreal Neurological Institute Z-axis coordinates are displayed. (B) Mean finite impulse response (FIR)-based predictor weights for Component 1 plotted as a function of poststimulus time. * = $P < 0.05$, ** = $P < 0.005$, *** = $P < 0.001$. [Color figure can be viewed at wileyonlinelibrary.com]

contrasts revealed that the interaction was due to increased activity in controls relative to patients at the peak of activity, namely at the 5 s, $F(1, 106) = 6.43$, $P < 0.05$, 7 s, $F(1, 106) = 19.82$, $P < 0.001$, and 9 s, $F(1, 106) = 4.31$, $P < 0.05$, poststimulus time points (Fig. 2B). This network peaked late in the trial, following the response to the target stimulus. Based on this late peak, its spatial distribution, and its relation to Component 2 (see *Intercorrelation between Networks*) this network was labeled *Response Modulation*.

Component 2

The brain regions associated with Component 2 are displayed in Figure 3A, with anatomical descriptions in Table III. This network included activations in bilateral STG (BAs 22, 38, 42), supplementary motor area (BA 6) extending into ACC/PCC (BAs 24, 32, 23), left precentral gyrus (BA 4), bilateral insula (BAs 47, 48) and thalamus. Component 2's recruitment of the STG was more extensive than in Component 1, whereas the opposite was true for its

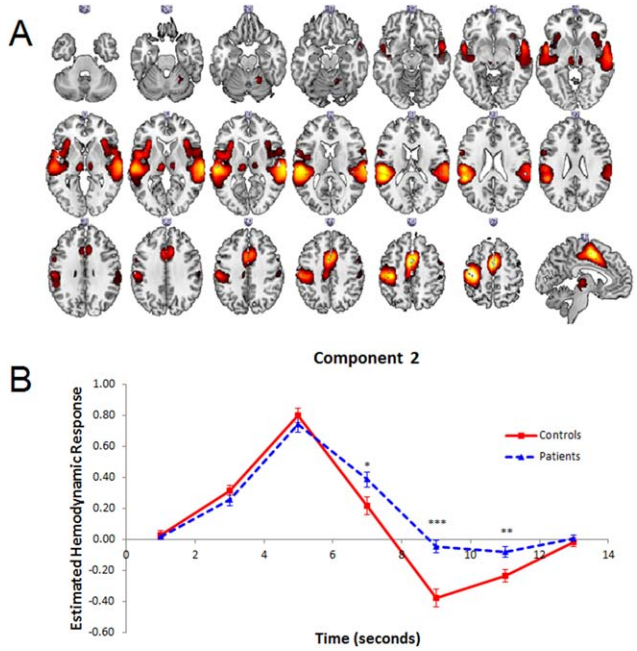

Figure 3.

(**A**, **B**) (A) Dominant 10% of component loadings for Component 2 Response Activation (blue/green = positive loadings, threshold = 0.09, max = 0.19; no negative loadings passed threshold) and Component 2 (blue/green = positive loadings, threshold = 0.04, max = 0.11; no negative loadings passed threshold). Overlapping regions are displayed in pink/white. Montreal Neurological Institute Z-axis coordinates are displayed. (B) Mean FIR-based predictor weights for Component 2 plotted as a function of poststimulus time. * = $P < 0.05$, ** = $P < 0.005$, *** = $P < 0.001$. [Color figure can be viewed at wileyonlinelibrary.com]

recruitment of the thalamus. As was the case for Component 1, Component 2 showed a significant Poststimulus Time × Group interaction, $F(6, 636) = 7.21$, $P < 0.001$, and a significant main effect of Group, $F(1, 106) = 7.67$, $P < 0.01$. Follow-up simple contrasts revealed that the interaction was due to increased activity in patients at the 7 s, $F(1, 106) = 5.25$, $P < 0.05$, 9 s, $F(1, 106) = 23.14$, $P < 0.001$, and 11 s, $F(1, 106) = 8.41$, $P < 0.005$, poststimulus time points (Fig. 3B). This network was labeled *Response Activation*, primarily due to its spatial distribution, which reflects other motor response networks identified in previous studies [Lavigne et al., 2015a; Metzak et al., 2012; Woodward et al., 2013].

Intercorrelation between Networks

In order to compute intercorrelations between networks, the pre-peak for Component 1 (*Response Modulation*) was computed as the mean of time points 3 and 4, and post-peak as the mean of time points 5, 6, and 7. For Component 2 (*Response Activation*), we computed pre-peak as the mean of time points 2 and 3, and post-peak as time points 4, 5, and 6. Intercorrelations of these measures resulted in high and negative correlations between Response Modulation pre-peak and Response Activation post-peak in both controls and patients, $r(48) = -0.62$, $P < 0.001$, $r(56) = -0.50$, $P < 0.001$, respectively. The difference between these correlations was not significant ($P = 0.38$ two-tailed). No other correlations were significant (all P's > 0.10). This suggests that participants who strongly activated the Response Modulation network subsequently strongly suppressed the Response Activation network.

Relation to Symptoms

In order to examine whether these significant group differences were associated with symptoms in the patient group, the networks' pre- and post-peak aggregate variables computed on the predictor weights were correlated with SAPS/SANS ratings in patients. Using a conservative P value of 0.01 as a cutoff for significance, only the association between delusions of reference and pre-peak activity in the response modulation network (Component 1) reached significance, $r(56) = -0.37$, $P < 0.005$ for global SAPS/SANS ratings and individual SAPS/SANS items.

Site Differences

Site differences were investigated by including Site as a between-subjects factor in the initial ANOVA, leading to a 7 × 2 × 2 × 5 mixed-model ANOVA with the within-subjects factors of Poststimulus Time (7) and Component (2), and the between-subjects factors of Group (2) and Site (5). The 4-way interaction was not significant ($P > 0.25$), nor were any other interactions involving Group and Site (all P's > 0.50), confirming consistency between sites with regard to group differences, and that these differences were not dependent on differences between the sites. However, there was a significant Component × Poststimulus Time × Site interaction, $F(24, 588) = 2.99$, $P < 0.001$. This interaction was explored by computing two 7 (Poststimulus Time) × 5 (Site) repeated-measures ANOVAs, one for each component, averaging across groups. For component 1 (*Response Modulation*), only the main effect of Poststimulus Time was significant, $F(6,618) = 24.78$, $P < 0.001$, indicating no site differences on activity within this network. For component 2 (*Response Activation*), both the main effect of Poststimulus Time, $F(6,618) = 132.95$, $P < 0.001$, and the Poststimulus Time × Site interaction, $F(24, 618) = 4.15$, $P < 0.001$, were significant. Simple contrasts were used to compare each site pair at each Poststimulus Time point, and these results are displayed in Table IV. These contrasts showed several patterns in the activity between sites: (1) MGH showed the least activity at stimulus onset (1 s) relative to all other sites except

TABLE II. Cluster volumes for the most extreme 10% of component loadings for Component 1 (Response Modulation) with anatomical descriptions, Montreal Neurological Institute (MNI) coordinates, and Brodmann's area (BA) for the peaks within each cluster

Brain regions	Cluster volume (voxels)	BA for peak locations	MNI coordinates		
			x	*y*	*z*
Cluster 1: Bilateral	24,450				
Cerebellum Crus I		n/a	−26	−76	−26
Cerebellum Crus I		n/a	28	−76	−24
Cerebellum Vermis VI		n/a	4	−74	−14
Cerebellum VI		n/a	22	−68	−22
Cerebellum I−IV		n/a	0	−48	0
Cerebellum Vermis Crus II		n/a	2	−76	−36
Cerebellum VIIIa		n/a	6	−70	−46
Thalamus		n/a	−8	−8	8
Thalamus		n/a	8	−6	8
Cerebellum VI		n/a	−24	−58	−20
Putamen		n/a	−28	−24	0
Lingual gyrus		18	−4	−64	−4
Cerebellum VIIIb		n/a	28	−44	−50
Hippocampus		n/a	−18	−24	−10
Precuneus		5	−6	−52	72
Precuneus		19	0	−82	40
Hippocampus		30	20	−22	−12
Hippocampus		30	18	−24	−10
Cerebellum V		n/a	28	−38	−36
Occipital pole		17	−4	−98	−4
Caudate		n/a	20	6	20
Cerebellum V		n/a	−22	−38	−28
Cerebellum VIIIa		n/a	−26	−44	−48
Supracalcarine cortex		18	0	−88	10
Precuneus		7	−2	−68	58
Amygdala		34	−28	0	−12
Postcentral gyrus		4	6	−38	78
Cerebellum Crus II		n/a	40	−62	−46
Cerebellum Crus II		n/a	−42	−58	−46
Putamen		n/a	30	−20	−2
Precuneus		5	2	−48	52
Cerebellum IX		n/a	−10	−56	−42
Brain Stem		n/a	−10	−30	−34
Brain Stem		n/a	14	−32	−34
Cluster 2: Right Hemisphere	629				
Temporal pole		38	52	20	−14
Superior temporal gyrus, anterior division		48	64	−2	0
Cluster 3: Right Hemisphere	452				
Middle temporal gyrus, temporooccipital part		37	62	−56	4
Middle temporal gyrus, posterior division		21	66	−38	−8
Middle temporal gyrus, posterior division		20	64	−28	−12
Cluster 4: Left Hemisphere	438				
Temporal pole		38	−58	12	−8
Cluster 5: Left Hemisphere	224				
Supramarginal gyrus, posterior division		40	−46	−46	58
Cluster 6: Right Hemisphere	142				
Putamen		n/a	16	18	−6
Cluster 7: Bilateral	126				
Cingulate gyrus, anterior division		24	0	30	30
Cluster 8: Right Hemisphere	119				
Amygdala		34	28	0	−14

TABLE II. (continued).

Brain regions	Cluster volume (voxels)	BA for peak locations	MNI coordinates		
			x	*y*	*z*
Cluster 9: Left Hemisphere	96				
Central opercular cortex		42	−62	−22	14
Cluster 10: Right Hemisphere	77				
Superior parietal lobule		2	46	−42	60
Cluster 11: Bilateral	68				
Cingulate gyrus, posterior division		23	0	−36	26

Yale; (2) UNM and Yale had a slower rise to peak (3 s), but not necessarily a lower peak, than the other three sites; (3) BWH showed the highest peak (5 s), which was significantly higher than all sites except MGH; and (4) Duke/UNC had a quicker return to baseline activity (7 s) than all other sites. Although these differences emerged in terms of degree of activity, all sites showed a similar time-course over the course of the trial, and site differences did not affect interpretation of the group results. See Figure 4A and 4B for site specific HDR shapes for Components 1 and 2, respectively.

DISCUSSION

In the current study, we acquired data from the fBIRN multisite collaboration auditory oddball task to investigate the functional brain networks related to auditory target detection in schizophrenia patients and healthy controls. We used fMRI-CPCA to identify networks that were specifically associated with the onset of target stimuli. Two functional brain networks emerged that showed differences between schizophrenia patients and healthy controls. The first network, on which patients showed reduced activity at the peak relative to controls, included temporal pole, MTG, ACC/PCC, parietal cortex, and several subcortical regions, including thalamus, striatum, hippocampus, and amygdala. The second network reflected a more generalized auditory–motor network, with activations in primary and secondary sensory regions, as well as bilateral insula, ACC, and thalamus. Although there was no difference between patients and controls at peak, patients demonstrated more sustained activation of this network, reflected as a slower return to baseline from peak. This sustained activity is in line with the behavioral findings of longer RTs and more late responses in the patient group. Importantly, activity from baseline to peak in component 1 was significantly correlated with activity from peak to baseline in component 2, whereby participants who showed a greater rise to peak in component 1 showed a faster post-peak return to baseline in component 2, interpreted as playing a role in suppressing activity in the auditory–motor network. Overall, the results highlight impaired activity in a subcortical-dominant response modulation network in schizophrenia patients associated with sustained activation of a cortical auditory–motor network, which may underlie poorer performance during auditory oddball tasks.

Component 1 reflected a distributed network of activations, in temporal pole, anterior and posterior cingulate cortex, occipital cortex, supramarginal gyrus, thalamus, hippocampus, amygdala, and striatum. Impaired activity in subcortical regions in schizophrenia patients has been previously reported for auditory oddball tasks [Kiehl et al., 2005a]; however, the current study identifies the relevant functional brain network. Comparing these activations to the recent resting-state 7-network parcellation [Buckner et al., 2011; Choi et al., 2012; Yeo et al., 2011], activations spanned several networks, most notably, the sensorimotor (e.g., temporal pole), visual (e.g., occipital cortex), frontoparietal (e.g., supramarginal gyrus), and dorsal attention (e.g., MTG) networks. The extensive activation of the cerebellum spanned all of these networks. In contrast, the activations for component 2 (*Response Activation*) overlapped with only the sensorimotor (STG, SMA, precentral gyrus), and ventral attention (ACC, insula) networks. The strong negative correlation in both groups between the pre-peak of the first network and subsequent post-peak of the second network, suggests the first network was involved in modulating or facilitating the return to baseline of activity in the motor activation network; hence, the label *Response Modulation network*. Efficient execution of oddball tasks requires both initiation and subsequent suppression of a response during target trials. Each target trial involves executing a motor response, immediately followed by suppressing that response, and maintenance of this state until the next trial on which a response is required. Such motor control or response modulation involves coordinated activation of the direct and indirect pathways of the basal ganglia [Albin et al., 1989; Alexander et al., 1990; Calabresi et al., 2014]. Given the extensive activation of subcortical areas in this network, including striatum, this modulation may occur through the indirect pathway of the basal ganglia, in which increased striatal activity causes increased GABA-ergic tone in the thalamus, and reduced activation from the thalamus to the motor cortex, allowing for motor control. Dysfunctional interaction between these two pathways has most notably been linked to movement disorders [DeLong and Wichmann,

TABLE III. Cluster volumes for the most extreme 10% of component loadings for Component 2 (Response Activation) with anatomical descriptions, Montreal Neurological Institute (MNI) coordinates, and Brodmann's area (BA) for the peaks within each cluster

Brain regions	Cluster volume (voxels)	BA for peak locations	MNI coordinates		
			x	*y*	*z*
Cluster 1: Left Hemisphere	17,138				
Precentral gyrus		4	−40	−20	58
Supplementary motor area		6	−2	2	52
Parietal operculum cortex		48	−54	−24	16
Planum Temporale		42	−52	−38	20
Planum Polare		38	−54	0	−4
Insular cortex		48	−32	18	6
Precentral gyrus		6	−58	6	24
Planum Polare		48	−40	−18	−4
Cingulate gyrus, posterior division		23	−12	−24	42
Cluster 2: Right Hemisphere	8,244				
Superior temporal gyrus, posterior division		22	64	−24	8
Superior temporal gyrus, anterior division		38	56	2	−8
Insular cortex		47	34	22	2
Insular cortex		48	40	10	0
Postcentral gyrus		3	54	−20	42
Cluster 3: Left Hemisphere	464				
Thalamus		n/a	−10	−20	4
Cluster 4: Right Hemisphere	323				
Precentral gyrus		6	52	2	46
Cluster 5: Right Hemisphere	317				
Thalamus		n/a	10	−18	2
Cluster 6: Right Hemisphere	290				
Cerebellum V		n/a	20	−52	−24
Cluster 7: Left Hemisphere	56				
Intracalcarine cortex		17	−6	−76	8

2007], but also has implications for schizophrenia, as this interaction is strongly modulated by dopamine and can be normalized using antipsychotic medication in mice [Cazorla et al., 2015]. The involvement of inferior frontal and parietal regions in this Response Modulation network may also contribute to the suppression of the motor response. This network also included activations in cerebellum, which is attenuated during auditory target detection in schizophrenia [Kiehl et al., 2005a; Kim et al., 2009], and is known to play a role in response inhibition [Picazio and Koch, 2015]. Interestingly, the magnitude of the activity in this network (including regions such as the striatum) was also correlated with the intensity of delusions of reference. This is consistent with the "aberrant salience" hypothesis [Kapur, 2003], as well as findings on the neural correlates of delusions of reference [Menon et al., 2011], which suggest that increased referential ideation might be related to difficulties with differentiating between self-relevant and irrelevant stimuli, and associated with increased activity within the subcortical striatal–limbic network.

In patients, activity in this network was decreased relative to controls, and was associated with longer and more sustained activity in the motor activation network, in line with the behavioral findings of longer reaction times and a greater number of late responses seen in this group. Previous research examining oculomotor control in schizophrenia has also reported similar findings. Dyckman et al. [2011] found that schizophrenia patients showed sustained activity in the frontal eye fields during performance of antisaccades, which require both response activation and inhibition. Similar to the current results, this sustained activity did not coincide with differences in the amplitude of activation at the peak. They also reported that this persistent activation was associated with increased latency to respond in subsequent trials. These and the current findings highlight the importance of examining not only spatial, but also temporal differences in functional brain activity, not only in terms of differences between groups, but also between networks themselves.

In addition to distinct activations, both networks showed activations in overlapping regions, in bilateral temporal cortex, ACC, and thalamus. Activity in overlapping regions in two orthogonal networks can be difficult to interpret, especially when these demonstrate opposing hemodynamic response patterns across groups, as was the case in the current study. As others have noted [Kim et al., 2009], seemingly overlapping activations across two or more functional brain networks likely reflect functional

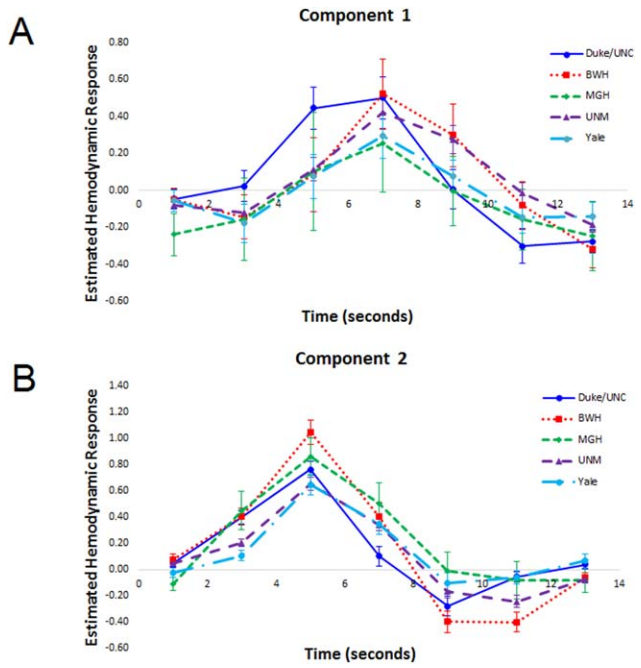

Figure 4.

(**A**, **B**) (A) Mean finite impulse response (FIR)-based predictor weights for Component 1 (Response Modulation) plotted as a function of site. (B) Mean FIR-based predictor weights for Component 2 (Response Activation) plotted as a function of site. [Color figure can be viewed at wileyonlinelibrary.com]

subsystems occupying the same broad region. This has certainly already been proposed for thalamus [Mitchell et al., 2014; Sherman, 2012] and ACC [Torta and Cauda, 2011; Yu et al., 2011], and there is evidence that sensory processing regions, including auditory cortex, might also serve this purpose during auditory target detection [Kim et al., 2009]. Therefore, although several brain regions showed overlapping and opposing activations across both networks, this likely reflects important subdivisions within these regions that inform each network separately and show distinct group differences. For example, the role of the thalamus in informing the response modulation network was attenuated in patients, while this was not the case with regard to its contributions to the peak of the response activation network. This distinction is an important one to consider when multiple overlapping functional brain networks are observed.

TABLE IV. Results of simple contrasts for the ANOVA between poststimulus time and site for component 2

	Poststimulus time point (seconds)						
Site comparison	**1**	**3**	**5**	**7**	**9**	**11**	**13**
Duke/UNC vs. BWH			↓*	↓*		↑***	
Duke/UNC vs. MGH	↑*			↓*			
Duke/UNC vs. UNM		↑**		↓**		↑*	↑*
Duke/UNC vs. Yale		↑***		↓**			
BWH vs. MGH	↑*				↓*	↓*	
BWH vs. UNM		↑*	↑**				
BWH vs. Yale		↑**	↑*		↓*	↓***	
MGH vs. UNM	↓*	↑*					
MGH vs. Yale		↑**					
UNM vs. Yale						↓*	

Arrows denote higher or lower activity as indicated. * = $P < 0.05$; ** = $P < 0.005$; *** = $P < 0.001$.

An important consideration when interpreting the results of oddball tasks is that it is not possible to distinguish between functional brain activity underlying target/salience detection and that which reflects responding, since responses are only required to target stimuli. Our motor activation network reflects this confound, as it includes regions from both the sensorimotor (i.e., precentral gyrus, SMA, STG, thalamus) and ventral attention (i.e., ACC, insula) networks, the latter of which has been strongly implicated in target detection [Kim, 2014]. It is, therefore, difficult to determine whether the differences between patients and controls stem from impairments in target detection, auditory–motor processing, or some combination of the two. Thus, motor response-based and salience-based interpretations of these results are equally valid. Given the widespread distribution of what we've interpreted as a response modulation network, it might reflect a combination of multiple, interacting subsystems not unlike our response activation network, which also includes nodes of the ventral attention network. For example, the striatum, thalamus, and cerebellum may be part of a motor-related subsystem, while regions such as the amygdala, hippocampus, and temporal pole, which are strongly interconnected [Chabardes et al., 2002], may form a second subsystem that interacts with the motor subsystem and has similar temporal hemodynamics during an oddball task. Although regions such as the amygdala and hippocampus are commonly active during oddball tasks, their exact role has not been thoroughly explored. A potential way of further teasing apart these subsystems is to implement more complex versions of oddball tasks, such as having participants respond to both target and non-target stimuli using different response buttons.

Utilization of data from multiple sites has several strengths. Data collaboration projects such as fBIRN facilitate the analysis of larger samples, allowing for a more thorough investigation of subject-specific factors, such as symptoms. However, multisite studies also introduce several potential confounds, including differences in scanners and scanning parameters, which may lead to noisier data. Due to these differences, certain sites may contribute more or less strongly to the results. Thus, the importance of quality control procedures prior to and during data collection, as well as examination of between site differences during analysis, must be given consideration. The fBIRN

consortium implemented various quality control procedures, ensuring as much consistency between sites as possible in terms of scanning parameters and experimental design [Glover et al., 2012]. In our study, we investigated whether site differences influenced our results by including Site as a between-subjects factor. We found no significant interactions between Site and Group, indicating that the group differences identified were consistent across sites. However, there were differences between sites in terms of degree of activation in our second component (response activation). For example, the higher peak in data from BWH relative to almost all other sites suggests that this site contributed more strongly to results on this component. However, the group-based results we found occurred during the decrease from peak back to baseline, where only Duke/UNC differed from the other sites, showing decreased activity. It is difficult to determine whether one or more sites contributed more strongly to the results than others. Although the lack of interaction between Group and Site suggests this was not the case in the current study, differences between sites need to be carefully considered when analyzing multisite data. Presently, it is not clear what differences contributed to the site differences identified, as there was no obvious distinction between activity at different scanner strengths, and scanning parameters were generally consistent. Future research using data from multiple sites should carefully examine these potential confounds.

A benefit of publicly available data sharing projects is that they allow for multiple research teams to conduct independent analyses on the same dataset. Kim et al. [2009] examined functional brain networks underlying auditory oddball using an overlapping sample of the fBIRN dataset, and reported widespread hypoactivity in patients in several auditory and prefrontal networks. Comparison of their findings with those of the current study show some overlap (e.g., decreased activity in patients within temporal cortex, ACC, cerebellum, and thalamus), but also highlight differences likely borne out of the distinct analysis techniques used. Notably, other than thalamus, no subcortical regions emerged on the networks identified in that study, which is a striking departure from the current findings. We also did not observe any substantial networks involving prefrontal cortex or the default mode. Although both studies utilized multivariate methods to identify functional brain networks underlying auditory target detection in an overlapping dataset, Kim et al. [2009] employed ICA, which derives networks from overall brain activity, whereas the method used in the current study, fMRI-CPCA, optimizes the analysis to detect task-related brain networks. Therefore, networks identified through ICA will capture primarily task-timing-unrelated variance, and may not match those reported here, and instead may be more similar to resting-state networks that are dysfunctional in patients and unaffected first-degree relatives [Chang et al., 2014]. However, it should be noted that although both studies used overlapping samples, there were no significant differences between groups on accuracy or reaction times in the previous study [Kim et al., 2009], which raises the possibility that differences between the samples may also have contributed to the different networks identified.

Although our use of a large, publicly available dataset resulted in a relatively large sample size, allowing for examination of associations with symptoms, a limitation of this study is that the potential confound of medication was not addressed. It is possible that medication effects may underlie the differences seen between groups in terms of more efficient recruitment of subcortical regions, especially considering some preclinical research suggests antipsychotics may influence the balance between the direct and indirect motor pathways. In addition, the patient group included diagnoses of both schizophrenia and schizoaffective disorder, and although these are often combined in research on psychosis, there remains the possibility of distinct neurobiological pathologies between these disorders.

CONCLUSION

This set of results suggests that: (1) a response modulation network, which includes subcortical regions, showed decreased activity in patients relative to controls; and (2) this response modulation network plays a role in post-response suppression of an auditory–motor response network, and patients showed a slower return to baseline than controls on this network. (3) Baseline to peak activation of the response modulation network was negatively correlated with peak to baseline activity in the response activation network. (4) Patients' impaired activity in the response modulation network, and subsequent longer return to baseline in the response activation network, corresponds with their later and less accurate behavioral performance, suggesting that this impairment in suppression of the auditory–motor response activation network could be an important aspect of oddball deficits in schizophrenia. (5) The magnitude of the activity in the response modulation network was correlated with the intensity of delusions of reference, supporting the notion that increased referential ideation is associated with hyperactivity within the subcortical striatal-limbic network. These findings support accounts of schizophrenia highlighting the importance of subcortical regions in task performance and symptom severity, and demonstrate how multivariate exploratory data analysis techniques can provide a powerful tool for studying the relationship between functional brain networks in schizophrenia.

ACKNOWLEDGMENTS

Data used for this study were downloaded from the Function BIRN Data Repository (http://fbirnbdr.birncommunity.org:8080/BDR/), supported by grants to the Function

BIRN (U24-RR021992) Testbed funded by the National Center for Research Resources at the National Institutes of Health, U.S.A.

REFERENCES

Albin RL, Young AB, Penney JB (1989): The functional anatomy of basal ganglia disorders. Trends Neurosci 12:366–375.

Alexander GE, Crutcher MD, DeLong MR (1990): Basal ganglia-thalamocortical circuits: Parallel substrates for motor, oculomotor, "prefrontal" and "limbic" functions. Prog Brain Res 85:119–146.

Andreasen NC (1984a): Scale for the Assessment of Negative Symptoms (SANS). Iowa City, IA: University of Iowa.

Andreasen NC (1984b). Scale for the Assessment of Positive Symptoms (SAPS). Iowa City, IA: University of Iowa.

Blair JR, Spreen O (1989): Predicting premorbid IQ: A revision of the National Adult Reading Test. Clin Neuropsychol 3:129–136.

Buckner RL, Andrews-Hanna JR, Schacter DL (2008): The brain's default network. Ann N Y Acad Sci 1124:1–38.

Buckner RL, Krienen FM, Castellanos A, Diaz JC, Yeo BT (2011): The organization of the human cerebellum estimated by intrinsic functional connectivity. J Neurophysiol 106:2322–2345.

Cacciaglia R, Escera C, Slabu L, Grimm S, Sanjuán A, Ventura-Campos N, Ávila C (2015): Involvement of the human midbrain and thalamus in auditory deviance detection. Neuropsychologia 68:51–58.

Calabresi P, Picconi B, Tozzi A, Ghiglieri V, Di Filippo M (2014): Direct and indirect pathways of basal ganglia: A critical reappraisal. Nat Neurosci 17:1022–1030.

Calhoun VD, Adali T, Giuliani NR, Pekar JJ, Kiehl KA, Pearlson GD (2006): Method for multimodal analysis of independent source differences in schizophrenia: Combining gray matter structural and auditory oddball functional data. Hum Brain Mapp 27:47–62.

Cattell RB (1966): The screen test for the number of factors. Multivar Behav Res 1:245–276.

Cattell RB, Vogelmann S (1977): A comprehensive trial of the scree and kg criteria for determining the number of factors. Multivar Behav Res 12:289–325.

Cazorla M, Kang UJ, Kellendonk C (2015): Balancing the basal ganglia circuitry: A possible new role for dopamine D2 receptors in health and disease. Mov Disord 30:895–903.

Chabardes S, Kahane P, Minotti L, Hoffmann D, Benabid AL (2002): Anatomy of the temporal pole region. Epileptic Disord 4:S9–S15.

Chang X, Shen H, Wang L, Liu Z, Xin W, Hu D, Miao D (2014): Altered default mode and fronto-parietal network subsystems in patients with schizophrenia and their unaffected siblings. Brain Res 1562:87–99.

Choi EY, Yeo BT, Buckner RL (2012): The organization of the human striatum estimated by intrinsic functional connectivity. J Neurophysiol 108:2242–2263.

Corbetta M, Shulman GL (2002): Control of goal-directed and stimulus-driven attention in the brain. Nat Rev Neurosci 3: 201–215.

DeLong MR, Wichmann T (2007): Circuits and circuit disorders of the basal ganglia. Arch Neurol 64:20–24.

Dyckman KA, Lee AKC, Agam Y, Vangel M, Goff DC, Barton JJS, Manoach DS (2011): Abnormally persistent fMRI activation during antisaccades in schizophrenia: A neural correlate of perseveration? Schizophr Res 132:62–68.

First M, Spitzer R, Gibbon M (2002a): Structure Clinical Interview for DSM-IV-TR Axis I Disorders-Non-Patient Edition (SCID-I/NP, 11/2002 revision). New York, NY: Biometric Research Department, New York State Psychiatric Institute.

First M, Spitzer R, Gibbon M, Williams J (2002b): Clinical Interview for DSM-IV-TR Axis I Disorders, Research Version, Patient Edition (SCID-I/P). New York: New York State Psychiatric Institute.

Fox MD, Snyder AZ, Vincent JL, Corbetta M, Van Essen DC, Raichle ME (2005): The human brain is intrinsically organized into dynamic, anticorrelated functional networks. Proc Natl Acad Sci U S A 102:9673–9678.

Friedman L, Glover GH, Fbirn C (2006a): Reducing interscanner variability of activation in a multicenter fMRI study: Controlling for signal-to-fluctuation-noise-ratio (SFNR) differences. NeuroImage 33:471–481.

Friedman L, Glover GH, Krenz D, Magnotta V (2006b): Reducing inter-scanner variability of activation in a multicenter fMRI study: Role of smoothness equalization. NeuroImage 32:1656–1668.

Friedman L, Stern H, Brown GG, Mathalon DH, Turner J, Glover GH, Gollub RL, Lauriello J, Lim KO, Cannon T, Greve DN, Bockhol HJ, Belger A, Mueller B, Doty MJ, He J, Wells W, Smyth P, Pieper S, Kim S, Kubicki M, Vangel M, Potkin SG (2008): Test-retest and between-site reliability in a multicenter fMRI study. Hum Brain Mapp 29:958–972.

Garrity AG, Pearlson GD, McKiernan K, Lloyd D, Kiehl KA, Calhoun VD (2007): Aberrant "default mode" functional connectivity in schizophrenia. Am J Psychiatry 164:450–457.

Glover GH, Mueller BA, Turner JA, van Erp TGM, Liu TT, Greve DN, Voyvodic JT, Rasmussen J, Brown GG, Keator DB, Calhoun VD, Lee HJ, Ford JM, Mathalon DH, Diaz M, O'Leary DS, Gadde S, Preda A, Lim KO, Wible CG, Stern HS, Belger A, McCarthy G, Ozyurt B Potkin SG, Fbirn (2012): Function biomedical informatics research network recommendations for prospective multi-center functional magnetic resonance imaging studies. J Magn Reson Imaging 36:39–54.

Gur RE, Turetsky BI, Loughead J, Snyder W, Kohler C, Elliott M, Pratiwadi R, Ragland JD, Bilker WB, Siegel SJ, Kanes SJ, Arnold SE, Gur RC (2007): Visual attention circuitry in schizophrenia investigated with oddball event-related functional magnetic resonance imaging. Am J Psychiatry 164:442–449.

Hunter MA, Takane Y (2002): Constrained principal component analysis: Various applications. J Educ Behav Stat 27:105–145.

Jeon YW, Polich J (2003): Meta-analysis of P300 and schizophrenia: Patients, paradigms, and practical implications. Psychophysiology 40:684–701.

Kapur S (2003): Psychosis as a state of aberrant salience: A framework linking biology, phenomenology and pharmacology in schizophrenia. Am J Psychiatry 160:13–23.

Keator DB, Grethe JS, Marcus D, Ozyurt B, Gadde S, Murphy S, Pieper S, Greve D, Notestine R, Bockholt HJ, Papadopoulos P (2008): A National Human Neuroimaging Collaboratory Enabled by the Biomedical Informatics Research Network (BIRN). IEE Trans Inform Technol Biomed 12:162–172.

Kiehl KA, Liddle PF (2001): An event-related functional magnetic resonance imaging study of an auditory oddball task in schizophrenia. Schizophr Res 48:159–171.

Kiehl KA, Stevens MC, Celone K, Kurtz M, Krystal JH (2005a): Abnormal hemodynamics in schizophrenia during an auditory oddball task. Biol Psychiatry 57:1029–1040.

Kiehl KA, Stevens MC, Laurens KR, Pearlson G, Calhoun VD, Liddle PF (2005b): An adaptive reflexive processing model of

neurocognitive function: Supporting evidence from a large scale (n = 100) fMRI study of an auditory oddball task. NeuroImage 25:899–915.

Kim H (2014): Involvement of the dorsal and ventral attention networks in oddball stimulus processing: A meta-analysis. Hum Brain Mapp 35:2265–2284.

Kim DI, Mathalon DH, Ford JM, Mannell M, Turner JA, Brown GG, Belger A, Gollub R, Lauriello J, Wible C, O'Leary D, Lim K, Toga A, Potkin SG, Birn F, Calhoun VD (2009): Auditory oddball deficits in schizophrenia: An independent component analysis of the fMRI multisite function BIRN study. Schizophr Bull 35:67–81.

Lavigne KM, Metzak PD, Woodward TS (2015a): Functional brain networks underlying detection and integration of disconfirmatory evidence. Neuroimage 112:138–151.

Lavigne KM, Rapin LA, Metzak PD, Whitman JC, Jung K, Dohen M, Loevenbruck H, Woodward TS (2015b): Left-dominant temporal-frontal hypercoupling in schizophrenia patients with hallucinations during speech perception. Schizophr Bull 41:259–267.

Magnotta VA, Friedman L (2006): Measurement of signal-to-noise and contrast-to-noise in the fbirn multicenter imaging study. J Digit Imaging 19:140–147.

Mangalathu-Arumana J, Beardsley SA, Liebenthal E (2012): Within-subject joint independent component analysis of simultaneous fMRI/ERP in an auditory oddball paradigm. NeuroImage 60:2247–2257.

Menon M, Schmitz TW, Anderson AK, Graff A, Korostil M, Mamo D, Gerretsen P, Addington J, Remington G, Kapur S (2011): Exploring the neural correlates of delusions of reference. Biol Psychiatry 70:1127–1133.

Metzak PD, Feredoes E, Takane Y, Wang L, Weinstein S, Cairo T, Ngan ETC, Woodward TS (2011): Constrained principal component analysis reveals functionally connected load-dependent networks involved in multiple stages of working memory. Hum Brain Mapp 32:856–871.

Metzak PD, Riley JD, Wang L, Whitman JC, Ngan ETC, Woodward TS (2012): Decreased efficiency of task-positive and task-negative networks during working memory in schizophrenia. Schizophr Bull 38:803–813.

Mitchell AS, Sherman SM, Sommer MA, Mair RG, Vertes RP, Chudasama Y (2014): Advances in understanding mechanisms of thalamic relays in cognition and behavior. J Neurosci 34: 15340–15346.

Mulert C, Jäger L, Schmitt R, Bussfeld P, Pogarell O, Möller HJ, Juckel G, Hegerl U (2004): Integration of fMRI and simultaneous EEG: Towards a comprehensive understanding of localization and time-course of brain activity in target detection. NeuroImage 22:83.

Picazio S, Koch G (2015): Is motor inhibition mediated by cerebello-cortical interactions? Cerebellum 14:47–49.

Raichle ME, MacLeod AM (2001): A default mode of brain function. Proc Natl Acad Sci U S A 98:676.

Sakoglu U, Pearlson GD, Kiehl KA, Wang YM, Michael AM, Calhoun VD (2010): A method for evaluating dynamic functional network connectivity and task-modulation: Application to schizophrenia. Magma (New York, N.Y.) 23: 351–366.

Serences JT (2004): A comparison of methods for characterizing the event-related BOLD timeseries in rapid fMRI. NeuroImage 21:1690.

Sherman SM (2012): Thalamocortical interactions. Curr Opin Neurobiol 22:575–579.

Soltani M, Knight RT (2000): Neural origins of the P300. Crit Rev Neurobiol 14:199–224.

Takane Y, Shibayama T (1991): Principal component analysis with external information on both subjects and variables. Psychometrika 56:97–120.

Torta DM, Cauda F (2011): Different functions in the cingulate cortex, a meta-analytic connectivity modeling study. NeuroImage 56:2157–2172.

Woodward TS, Feredoes E, Metzak PD, Takane Y, Manoach DS (2013): Epoch-specific functional networks involved in working memory. NeuroImage 65:529–539.

Woodward TS, Leong K, Sanford N, Tipper CM, Lavigne KM (2016): Altered balance of functional brain networks in Schizophrenia. Psychiatry Res 248:94–104.

Wynn JK, Jimenez AM, Roach BJ, Korb A, Lee J, Horan WP, Ford JM, Green MF (2015): Impaired target detection in schizophrenia and the ventral attentional network: Findings from a joint event-related potential-functional MRI analysis. Neuroimage Clin 9:95–102.

Yeo BT, Krienen FM, Sepulcre J, Sabuncu MR, Lashkari D, Hollinshead M, Roffman JL, Smoller JW, Zollei L, Polimeni JR, Fischl B, Liu H, Buckner RL (2011): The organization of the human cerebral cortex estimated by intrinsic functional connectivity. J Neurophysiol 106:1125–1165.

Yu C, Zhou Y, Liu Y, Jiang T, Dong H, Zhang Y, Walter M (2011): Functional segregation of the human cingulate cortex is confirmed by functional connectivity based neuroanatomical parcellation. NeuroImage 54:2571–2581.